A Comparison of the Aerosol Thickness Derived from Ground-Based and Airborne Measurements

S. Kato
Hampton University
Hampton, Virginia

M. H. Bergin
Georgia Institute of Technology
Atlanta, Georgia

N. S. Laulainen and D. D. Turner
Pacific Northwest National Laboratory
Richland, Washington

T. P. Ackerman and E. E. Clothiaux
The Pennsylvania State University
University Park, Pennsylvania

G. G. Mace
University of Utah
Salt Lake City, Utah

T. P. Charlock and R. A. Ferrare
National Aeronautics and Space Administration
Langley Research Center
Hampton, Virginia

J. J. Michalsky
State University of New York at Albany
Albany, New York

Introduction

The extinction optical thickness of the atmosphere can be computed by measuring the attenuation of direct solar radiation (DSR). The aerosol extinction optical thickness in selected wavelength regions by sun photometry (Shaw 1983) is the residual optical thickness after the molecular scattering optical thickness and the ozone and nitrogen dioxide absorption optical thicknesses are subtracted from the extinction optical thickness. Since there is no other absorber known to have large cross sections and high concentrations in the wavelength region coinciding with regions of large aerosol extinction cross sections, this appears to be a reasonable assumption. However, whether this residual optical thickness (aerosol optical thickness [AOT]) is equal to the extinction optical thickness of particles needs to be examined. Such comparison is crucial to understand aerosol optical properties and radiative transfer under clear-sky conditions.

For this reason, we compare the extinction optical thickness of particles estimated from vertical profiles of scattering and absorption coefficients measured by an airborne integrating nephelometer and particle/soot absorption photometer (PSAP) with the aerosol extinction optical thickness derived from a ground-based (GB) Multifilter Rotating Shadowband Radiometer (MFRSR) (Harrison et al. 1994). Few attempts have been made to compare these two optical thicknesses, largely because there are not many aircraft measurements collocated with GB measurements. In addition, the scattering coefficient of particles is typically measured under lower relative humidity (RH) rather than ambient conditions because of instrumental heating (Ogren et al. 1996; Bergin et al. 1997). Therefore, a humidity correction is necessary to the scattering coefficient measured by an integrating nephelometer.

Data

Aircraft Data

The Gulfstream-1 measured aerosol properties over the Southern Great Plains (SGP) central facility (CF) (Lat. 97.48W, Long. 36.69N, Alt. 318m) during intensive operational periods (IOPs) in April 1997 and September 1997. The aircraft flew successive horizontal legs at different altitudes. Each leg was approximately 5 km in length. The aircraft went up to an altitude of approximately 5 km in a stacked pattern before spiraling down over the CF. The lowest altitude at which the aircraft took measurements was approximately 100 m above the ground. The scattering coefficient was measured by an integrating nephelometer (TSI 3563, Anderson et al. 1996; Anderson and Ogren 1998; Heintzenberg and Charlson 1996) at the three wavelengths of 450 nm, 550 nm, and 700 nm. We estimate that the uncertainty in the measured scattering coefficient under dry conditions is less than 10%. During the April 1997 IOP, the integrating nephelometer experienced problems associated with the in-flight measurement of the scattering coefficients of filtered air (zeroing check). As a consequence, zero checks were performed only during pre- and post-flight. Therefore, we treat the difference between pre- and post-flight values (7.59 M m^{-1} at 550 nm) as an additional uncertainty in the measured scattering coefficient for April 14.

Surface Data

While the aircraft took measurements over the CF, GB instruments were operated at the site. The extinction optical thickness of the atmosphere was computed from the direct irradiance measured by a MFRSR at wavelengths of 415 nm, 499 nm, 610 nm, 665 nm, and 862 nm.

In order to compute the extinction optical thickness of aerosol from MFRSR data, we subtract an ozone absorption optical thickness that is based on data taken at Boulder, Colorado, by the Climate Monitoring and Diagnostic Laboratory (CMDL) of the National Oceanic and Atmospheric Administration (NOAA). The monthly mean column amounts of ozone were 348 DU and 273 DU for April and September 1997. We used an amount of 300 DU for August 1998. These ozone amounts correspond to the absorption optical thickness of approximately 0.01 at 500 nm. However, we do not consider the absorption optical thickness of nitrogen dioxide. The absorption optical thickness of nitrogen dioxide is no more than 0.01. We also neglect stratospheric aerosols. Based on this and the error in the calibration, we estimated that the uncertainty in the aerosol extinction optical thickness derived from the MFRSR is ±0.01.

The scattering coefficient was also measured at the CF by an integrating nephelometer (TSI 3563) at approximately 20% RH (Bergin et al. 1998). In addition to this integrating nephelometer, a second integrating nephelometer was installed in December 1998 to measure the scattering coefficient as a function of RH. This is done by controlling RH at upstream of the integrating nephelometer ranging from 40% to 90% using a procedure described by Rood et al. (1987).

The absorption coefficient at 565 nm is measured by a PSAP at the CF. Further, a Raman Lidar (Goldsmith et al. 1998) was operated during IOPs in September 1997 and August 1998. The Raman Lidar measures the extinction coefficients profile at 355 nm, which can be integrated with respect to

height in order to estimate the extinction optical thickness of aerosol at 355 nm. Among these data taken during IOPs in April 1997, September 1997, and August 1998, we select data taken on April 14, September 27, and September 29, 1997.

Results

Scattering Coefficient as a Function of Relative Humidity

Scattering coefficients were measured at lower RH than ambient conditions. The extinction optical thickness of particles integrated from the scattering and absorption coefficient, τ_p is given by

$$\tau_p(\lambda, RH) = \int_0^{5km} \left[\sigma_{sp}(\lambda, z)F_{sca}(\lambda, RH) + \sigma_{ap}(\lambda, z)F_{abs}(\lambda, RH)\right]dz \quad (1)$$

where σ_{sp} and σ_{ap} are the scattering and absorption coefficients, respectively, measured under dry conditions, F_{sca} and F_{abs} are the humidity corrections to these coefficients, and RH is the RH of the atmosphere (i.e., Hegg et al. 1997; Bergin et al. 1998). While we assume that F_{ans} is unity, we need to estimate F_{sca} in order to compute τ_p. F_{sca} depends on several factors including the size distribution and chemical composition of dry particles, as well as state of particles, which were not measured in our study. Therefore, we estimate F_{sca} using two integrating nephelometers operated under different RH conditions by

$$F_{sca}(\lambda, RH) = \frac{\sigma_{sp}(\lambda, RH)}{\sigma_{sp,ref}(\lambda)} \quad (2)$$

where σ_{sp} (λ,RH) and $\sigma_{sp,ref}(\lambda)$ is the scattering coefficient measured at wet and dry conditions, respectively. We use data taken at the surface from December 1998 to January 1999 to derive $F_{sca}(\lambda,RH)$. In order to correct the scattering coefficient measured by the aircraft, we sort $F_{sca}(\lambda,RH)$ using bins with a 5% RH increment for all three wavelengths (Figure 1). We then interpolate these values at the ambient RH for the correction.

We computed τ_p by applying these relations for F_{sca} in Eq. (1) when the ambient RH is greater than 50%. F_{sca} is based on data taken at the surface in winter, we assume that chemical components and size distribution of dry particles in the atmospheric column are similar to those at the surface for all seasons by applying this relation as a correction to the scattering coefficient measured aloft.

The April and September 1997 Case Study

We averaged the scattering coefficient measured by the integrating nephelometer equipped on the aircraft over each flight leg. The averaged scattering coefficient at 550 nm for three days shows that although the maximum scattering coefficient occurs in the boundary layer, scattering by particles in the

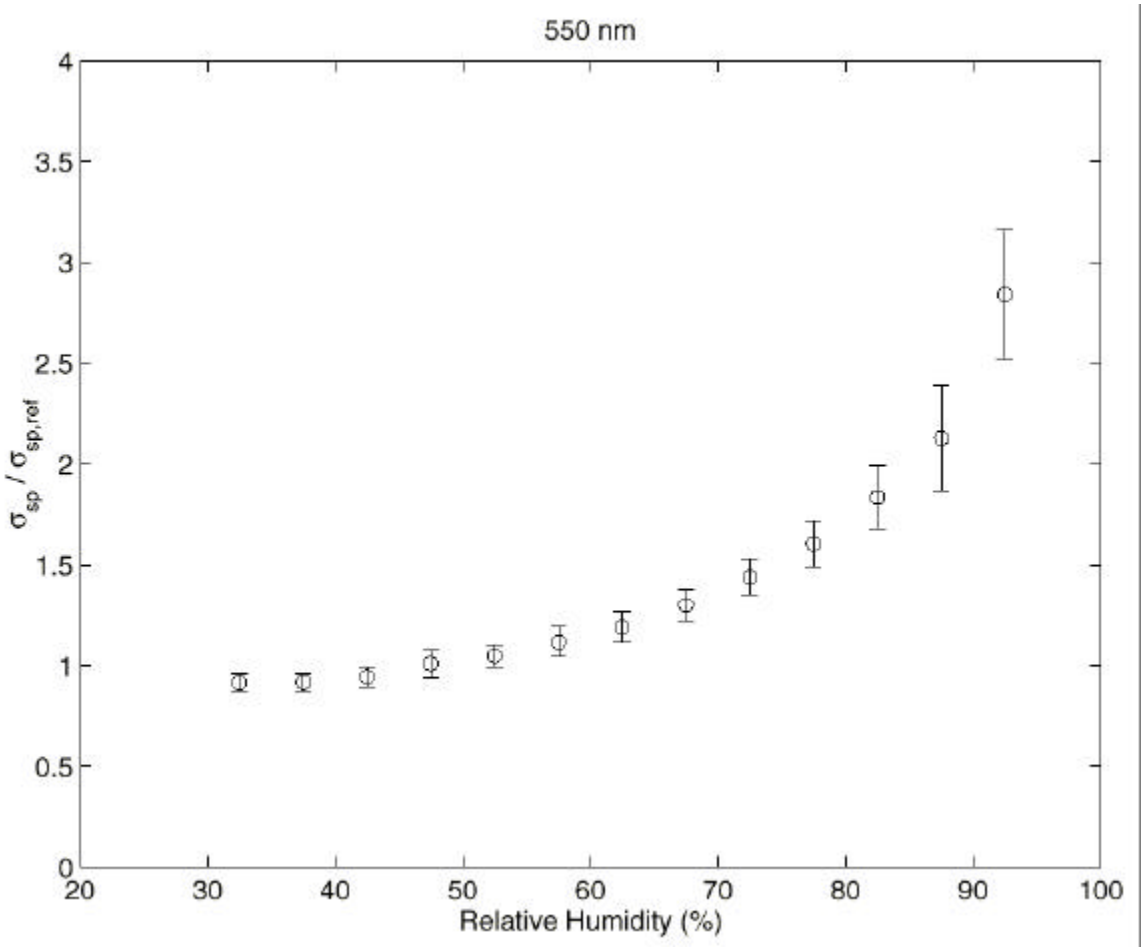

Figure 1. The ratio of the scattering coefficient measured under wet conditions to that measured under dry conditions as a function of the RH of wet conditions for the three wavelengths. The relation is obtained by fitting second order polynomials to data. Open circles and error bars indicate averaged values and standard deviations for every 5% RH intervals.

free troposphere is not negligible (Figure 2). The fraction of the scattering optical thickness by particles in the boundary layer to that in the entire column is approximately 0.4, 0.4, and 0.3 for April 14, September 27, and September 29, respectively.

The Raman Lidar operated at the CF measured the extinction coefficient at 355 nm. In order to compare the extinction coefficient derived from the Raman Lidar with the extinction coefficient of particles at 550 nm derived from the aircraft measurements, we scaled the extinction coefficient derived from the Raman Lidar, $\sigma_{sp,rl}$, by

$$\sigma_{sp,rl}(550) = \left(\frac{550}{355}\right)^{-1} \sigma_{sp,rl}(355) \qquad (3)$$

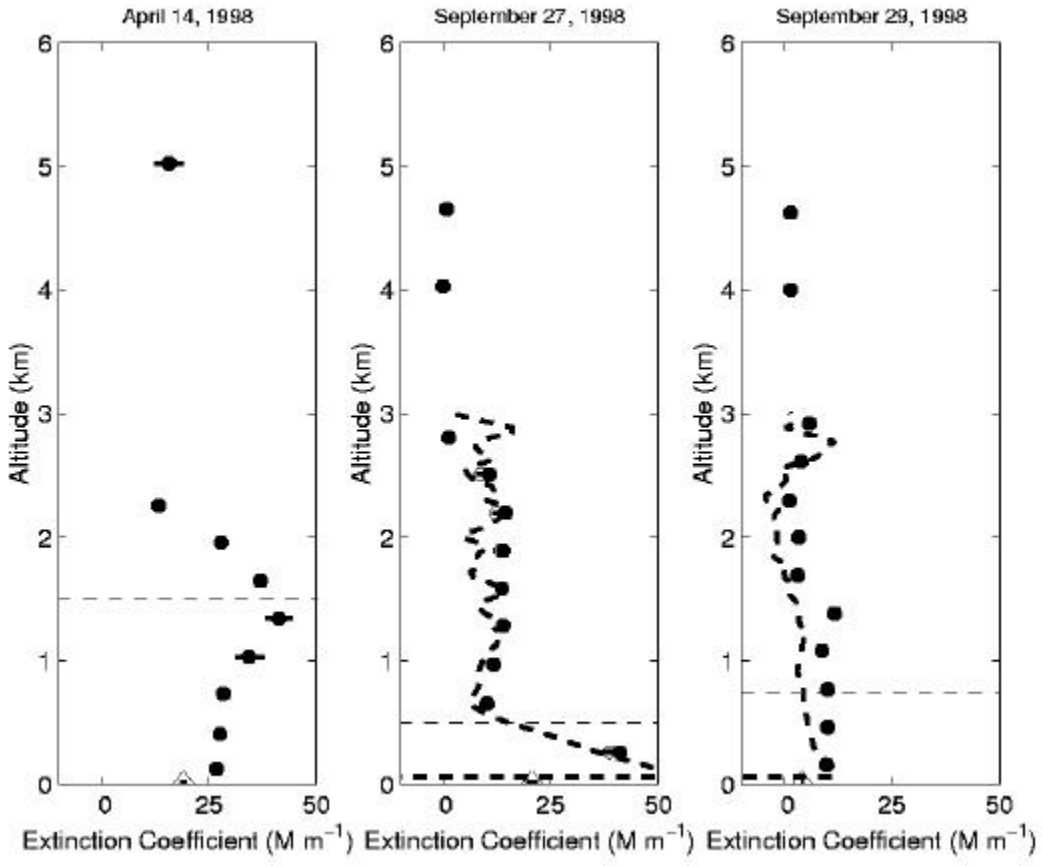

Figure 2. The extinction coefficients at 550 nm, which are the sum of the scattering coefficient measured by the integrating nephelometer and the absorption coefficient measured by the PSAP. Closed and open circles are with and without humidity corrections to the nephelometer data. Horizontal lines through the open circles indicate the standard deviation for each averaged value. The thin dashed line indicates the estimated height of the boundary layer. The thick dashed lines in September 1997 plots are the extinction coefficient profile at 550 nm estimated from the Raman Lidar averaged over each flight period.

where l is the exponent fitted to the AOT, τ, derived from the multifilter shadowband radiometer by the Lundholm relation

$$\tau = \alpha\lambda^{-l} \tag{4}$$

where λ is the wavelength.

In order to estimate the extinction optical thickness, τ_p, at 450 nm and 700 nm, we assume that the absorption coefficient is constant with wavelength; we use the absorption coefficient measured at 565 nm for the value at 450 nm and 700 nm. Comparisons of τ_p with the aerosol extinction optical thickness derived from the MFRSR (τ_{mfrsr} hereinafter) show that τ_p is smaller for the three days

(Figure 3). The differences at 550 nm are 0.01, 0.02, and 0.01 for April 14, September 27, and September 29, respectively, which correspond to 8%, 30%, and 31% of τ_{mfrsr}.

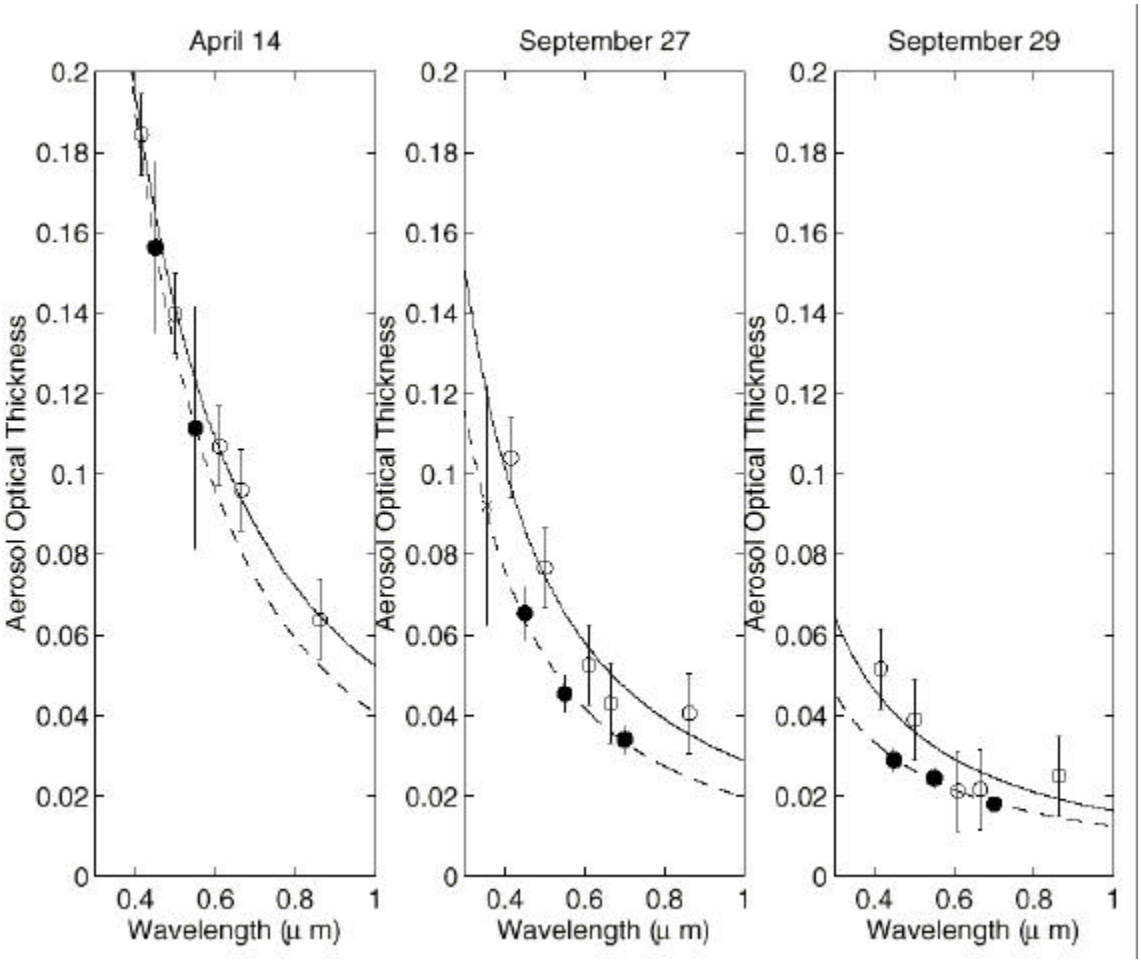

Figure 3. The aerosol extinction optional thickness obtained from the MFRSR (open circles) as a function of wavelength averaged over flight periods. Closed circles indicate the extinction optical thickness obtained by summing the particle scattering and absorption coefficients measured by the airborne integrating nephelometer and PSAP, respectively. The error bar indicates the estimated uncertainty in the nephelometer-derived extinction optical thickness and ±0.01 uncertainty for the MFRSR-derived extinction optical thickness. The solid and dashed lines are the result of fitting a Lundholm relation to the MFRSR and aircraft data, respectively. The extinction optical thickness derived from the Raman Lidar at 355 nm on September 27, 1997, is also plotted (x) with a vertical bar indicating the variation during the flight period.

Conclusion

We obtained the ratio of the scattering coefficient measured under wet and dry conditions as a function of RH, F_{sca}, from two integrating nephelometers operated under different RH conditions at the surface in order to correct the scattering coefficient measured by an airborne integrating nephelometer. The differences between the extinction optical thickness of particles, τ_p, and the aerosol extinction optical thickness derived from the MFRSR, τ_{mfrsr}, at 550 nm are 0.01, 0.02, and 0.01 for April 14, September 27, and September 29, respectively; τ_p is smaller for all three cases. If we take into account the uncertainties of both optical thicknesses, these differences are not significant.

Acknowledgments

We thank J. Ogren for useful advice regarding the instruments used for aircraft measurements; P. Daum, J. Hubbe, and V. Morris for supplying the aircraft data and for useful discussions regarding the accuracy of the data, and P. Wang for discussion regarding stratospheric aerosol. One of the authors (S. Kato) is supported by the National Aeronautics and Space Administration (NASA) Clouds and Earth's Radiant Energy System (CERES) grant NAG-1-1963. Work at Pacific Northwest National Laboratory (PNNL) was supported by the U.S. Department of Energy (DOE) under contract DE-ACD6-76RLO 1830. PNNL is operated for DOE by Battelle Memorial Institute. The work at the Pennsylvania State University was supported by the DOE Atmospheric Radiation Measurement (ARM) Program under grant DOE DE-FG02-90ER-61071.

References

Anderson, T. L., and J. A. Ogren, 1998: Determining aerosol radiative properties using the TSI3562 integrating nephelometer, aerosol. *Sci. Technol*., **29**, 57-69.

Anderson, T. L., et al., 1996: Performance characteristics of a high-sensitivity, three-wavelength, total/scatter/backscatter nephelometer. *J. Atmos. Oceanic. Technol*., **13**, 967-986.

Bergin, M. H., et al., 1998: Comparison of aerosol optical depth inferred from surface measurements with that determined by sun photometry for cloud-free conditions at a continental U.S. site. *J. Geophys. Res*. Submitted.

Bergin, M. H., J. A. Ogren, S. E. Schwartz, and L. M. McInnes, 1997: Evaporation of ammonium nitrate aerosol in a heated nephelometer: implication for field measurements. *Environ. Sci. Technol*., **31**, 2878-2883.

Goldsmith, J. E. M., F. H. Blair, S. E. Bisson, and D. D. Turner, 1998: Turn-key Raman Lidar for profiling atmospheric water vapor, clouds, and aerosol. *Appl. Opt*., **37**, 4979-4990.

Harrison, L., J. Michalsky, and J. Berdt, 1994: Automated multifilter rotating shadow-band radiometer: an instrument for optical depth and radiation measurements. *Appl. Opt*., **22**, 5118-5125.

Hegg, D. A., J. Livingston, P. V. Hobbs, T. Novakov, and P. Russel, 1997: Chemical apportionment of aerosol column optical depth off the mid-Atlantic coast of the United States. *J. Geophys. Res*., **102**, 25,293-25,303.

Heintzenberg, J. R., and J. Charlson, 1996: Design and application of the integrating nephelometer: a review. *J. Atmos. Ocean. Tech*., **13**, 987-1000.

Ogren, J. A., S. Anthony, J. Barnes, M. H. Bergin, W. Huang, L. M. McInnes, C. Myers, P. Sheridan, S. Thaxton, J. Wendell, 1996: Aerosol and radiation. *NOAA/Climate Monitoring and Diagnostic Laboratory Summary Report 1994-1995*.

Rood, M. D, D. S. Covert, and T. V. Larson, 1987: Hygroscopic properties of atmospheric aerosol in Riverside, California. *Tellus*, **39B**, 383-3971.

Shaw, G. E., 1983: Sun photometry. *Bull. Amer. Meteorol. Soc*., **64**, 4-10.